Proceedings of the Sixth International Conference on
Railway Technology: Research, Development and Maintenance
Edited by: J. Pombo
Civil-Comp Conferences, Volume 7, Paper 13.5
Civil-Comp Press, Edinburgh, United Kingdom, 2024
ISSN: 2753-3239, doi: 10.4203/ccc.7.13.5

Stochastic Track Vibration Analysis in Consideration of Log-Normal Type Spatial Variation of Rail Material Parameters and Shape Dimensions

K. Koro[1], K. Suzuki[2] and K. Abe[1]

[1] **Faculty of Engineering, Niigata University Japan**
[2] **School of Engineering, Niigata University Japan**

Abstract

We investigate the influence of random variables selection on spatial variation of rail material parameters and shape dimensions to the expected value and the standard deviation of the simulated track dynamic response. The spatial variation is considered about Young's modulus, density, cross-sectional area, moment of inertia and surface profile on a rail, using the Karhunen-Loève expansion. The random variables in the Karhunen-Loève expansion are chosen from the standard normal- or the standard log-normal random variables. The dynamic response in a probability space is evaluated using the polynomial chaos and the stochastic collocation method Through numerical tests, we investigate the expected value and the standard deviation of the three kinds of dynamic forces, the wheel-rail contact force, the railpad force and the sleeper-ballast force for several running speed of a wheel. The expected value and the standard deviation of the wheel-rail contact force increase with rise of the wheel running speed c, due to existance of rail surface profile. The dynamic behavior on the expected value and the standard deviation tends to be independent of the choice of the standard normal- or the standard log-normal random variables in Karhunen-Loève expansion.

Keywords: wheel-track vibration, spatial variation, material parameters and shape dimensions, Karhunen-Loeve expansion, log-normal random variable, polynomial chaos.

1 Introduction

A railway track is comprised of rail, sleeper, railpad, ballast, subballast and subgrade. The train passing on such a track is accompanied by wheel-track vibration, which leads to a track deterioration and train safety reduction. In a few decade, many simulation methods for wheel-track vibration have been proposed by e.g. [1, 2]. Most of the presented studies are based on the deterministic FE-based simulation, while the members have certain spatial variation on their material parameters and shape dimensions. [3–7]. The spatial variation in the input information propagates as uncertainties of the dynamic response in railway track. We thus requires the stochastic vibration analysis of railway track, for the progression of railway track design.

As the presented studies on the stochastic track vibration analysis, Andersen et al [8] have attempted to the vibration analysis on a track with elastic foundation with spatial varitation. Bressolette et al [9] have investigated the influence of the variation of elastic modulus and the thickness of a ballast layer to the static/dynamic response of a track. Rhayma et al [10] have simulated the dynamic response of a ballst track with the uncertainties of depths of ballast layer and subgrade. Sadri et al [11] have estimated the initiation and progression of track deterioration of a track with spatial variation of support stiffness. Nowadays, the authors have attemped the track vibration in consideration of spatial variation of ballast elastic modulus [12]. In the paper [13], we have considered the spatial variation of ballast elastic modulusand density in a stochastic analysis on track vibration. Moreover, we have investigated the influence of spatial variation of rail material parameters and shape dimensions to the dynamic response of track components [14]. In the ref. [14], the Karhunen-Loève expansions on rail uncertainties are defined using the standard normal random variables: the non-Gaussian type spatial variation of material parameters and shape dimensions of rail has not been considered in the stochastic simulation.

In the present paper, we investigate the influence of random variables selection on spatial variation of rail material parameters and shape dimensions to the expected value and the standard deviation of the simulated track dynamic response. The well known beam-mass-spring system [2] is used as the wheel-track vibration model. The spatial variation is considered about Young's modulus, density, cross-sectional area, moment of inertia and surface profile on a rail. The Karhunen-Loève (KL) expansion [15] is used for modeling the spatial variation of 4 rail parameters and the rail surface profile. We consider a choice of the random variables in the KL expansion, the standard normal- or the standard log-normal random variables. The dynamic response in a probability space is evaluated using the polynomial chaos (PC) [15] and the stochastic collocation method [16]. We now investigate the influence of a choice of random variables on spatial variation of rail material parameters and shape dimensions, to the expected value and the standard deviation of the similated results on wheel-rail contact force, railpad force and sleeper-ballast force.

2 Wheel-Track Vibration Model

In the present study, the wheel-track vibration phenomena is modeled as shown in Figure 1 [2]. A rail is modeled as a single, uniform and straight Bernoulli-Euler beam.

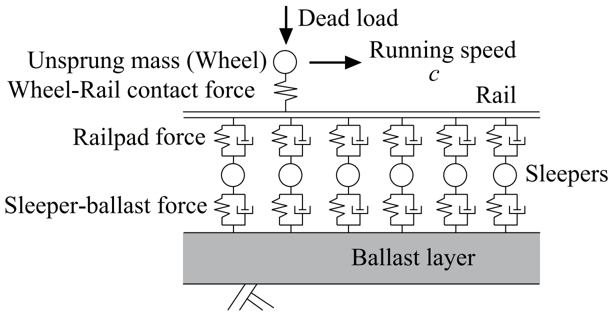

Figure 1: wheel-track vibration model.

The single beam is discretely supported by sleepers. The variational form of vertical motion of the rail is described as

$$\begin{aligned}\int_0^L E_r(x)I_r(x)\frac{\partial^2 u_r}{\partial x^2}(x,t)\frac{\partial^2 \delta u_r}{\partial x^2}(x)dx + \int_0^L \rho_r(x)A_r(x)\frac{\partial^2 u}{\partial t^2}(x,t)\delta u_r(x)dx \\ = \sum_{j=1}^{N_{wh}} \delta u_r(x_j + ct)P_j(t) - \sum_{j=1}^{N_{slp}} \delta u_r(a_j)F_j(t),\end{aligned} \tag{1}$$

where $u_r(x,t)$ is the rail deflection and $\delta u_r(x)$ is its variational components. E_r is rail Young's modulus, and ρ_r is the rail density. I_r and A_r are the moment of inertia and the area of rail cross-section, respectively. x is the longitudinal coorinate and t is the time. The railpad force $F_j(t)$ acting at the sleeper support $x = a_j$ is consequently modeled as a concentrated load.

The wheel-rail contact force $P_j(t)$, which is a moving concentrated load with the constant running speed c, is defined as

$$P_j(t) = k_c(u_{wh,j}(t) - u_r(x_j + ct, t) + X(x_j + ct)), \qquad (j = 1, 2, \ldots, N_{wh}) \tag{2}$$

where k_c is the spring constant of contact. $X(x_j + ct)$ is the surface profile at the contact point $x = x_j + ct$.

The wheels are modeled as unsprung masses, and the equations of their vertical motions are expressed as follows:

$$m_{wh,i}\frac{\partial^2 u_{wh,i}}{\partial t^2}(t) = P_{b,i} + m_{wh,i}g - P_i(t), \qquad (i = 1, 2, \ldots, N_{wh}) \tag{3}$$

where $u_{wh,i}(t)$ is the vertical displacement of the ith wheel with the mass $m_{wh,i}$. $P_{b,i}$ is a dead load.

The railpad force $F_j(t)$ is modeled with a Voigt unit as

$$F_j(t) = k_{rp}(u_{r,j}(a_j,t) - u_{slp,j}(t)) + \eta_{rp}(\dot{u}_{r,j}(a_j,t) - \dot{u}_{slp,j}(t)), \qquad (j = 1,2,\dots,N_{slp}) \tag{4}$$

where k_{rp} and η_{rp} are the spring constant and the damping coefficients of the railpads.

The vertical displacement $u_{slp,j}(t)$ on the jth sleeper with mass $m_{slp,i}$ is governed by the following equation of motions:

$$m_{slp,i}\frac{\partial^2 u_{slp,i}}{\partial t^2}(t) = F_{rp,i}(t) + m_{slp,i}g - F_{s,i}(t), \qquad (i = 1,2,\dots,N_{slp}). \tag{5}$$

The ith sleeper reaction force $F_{s,i}(t)$ is described as

$$F_{s,i}(t) = k_s(u_{slp,i}(t) - u_{b,i}(t)) + \eta_s(\dot{u}_{slp,i}(t) - \dot{u}_{b,i}(t)), \qquad (i = 1,2,\dots,N_{slp}) \tag{6}$$

where $u_{b,i}$ is the vertical displacement of ballast surface.

3 Simulation method for railway track vibration with spatial variation of rail material parameters and shape dimensions

In the present study, we consider spatial variation of 5 material parameters and shape dimensions of a rail: Young's modulus, density, cross-sectional area, moment of inertia and surface profile. The spatial variation of these parameters is described with Karhunen-Loève (KL) expansion. The dynamic response in a probability space is approximated with the polynomial chaos (PC) expansion. The PC expansion coefficients of dynamic response are then calculated using the deterministic simulation results and the stochastic collocation method.

3.1 Modeling of spatial variation of rail material parameters and shape dimensions

The spatial variation of Young's modulus $E_r(x)$, the density $\rho_r(x)$, the cross sectional area $A_r(x)$, the moment of inertia $I_r(x)$ and the rail surface profile $X(x)$ are defined with KL expansions [15] as

$$E_r(x) = \bar{E}_r(x) + \sum_{m=1}^{N_{KL}} \xi_{E,m} \sqrt{\lambda_{E,m}} f_{E,m}(x) \tag{7}$$

$$\rho_r(x) = \bar{\rho}_r(x) + \sum_{m=1}^{N_{KL}} \xi_{\rho,m} \sqrt{\lambda_{\rho,m}} f_{\rho,m}(x) \tag{8}$$

$$A_r(x) = \bar{A}_r(x) + \sum_{m=1}^{N_{KL}} \xi_{A,m} \sqrt{\lambda_{A,m}} f_{A,m}(x) \tag{9}$$

$$I_r(x) = \bar{I}_r(x) + \sum_{m=1}^{N_{KL}} \xi_{I,m} \sqrt{\lambda_{I,m}} f_{I,m}(x) \tag{10}$$

$$X(x) = \bar{X}(x) + \sum_{m=1}^{N_{KL}} \xi_{X,m} \sqrt{\lambda_{X,m}} f_{X,m}(x) \tag{11}$$

where $\lambda_{*,m}$ and $f_{*,m}$ are the eigenvalue and the eigenfunction of the covariance kernel $C(x; y)$ on spatial variation, respectively. An expected value is described with $^{-}$. N_{KL} is the number of terms in the truncated KL expansion.

$\xi_{E,m}$, $\xi_{\rho,m}$, $\xi_{A,m}$, $\xi_{I,m}$ and $\xi_{X,m}$ are standard normal random variables. If we choose standard log-normal random variables in Eqs.(7)-(11), we have to transform the random variables $\xi_{*,m}$ to into new variables $\eta_{*,m}$ as

$$\eta_{*,m} = \frac{e^{\xi_{*,m}} - \sqrt{e}}{\sqrt{e(e-1)}}. \tag{12}$$

The log-normal random variables $\eta_{*,m}$ have the orthogonality as [17]

$$\langle \eta_{*,i} \rangle = 0, \qquad \langle \eta_{*,i} \eta_{*,j} \rangle = \delta_{ij}, \tag{13}$$

where $\langle \cdot \rangle$ denotes the expectation operator, and δ_{ij} is the Kronecker delta.

3.2 Stochastic collocation method

In the presented papers, the railway dynamic response in a probability space have been simulated using Monte Carlo Simulation(MCS) or the spectral stochastic finite element method (SSFEM) [12]. The simulation with these methods requires large computational work, which is drawback for stochastic simulation with many random variables on wheel-track dynamics.

We now utilize the stochastic collocation method (SCM) [16] for evaluating the response of dynamic force in probability space. The SCM is based on the approximation in probability space with the polynomial chaos (PC) expansion [15]. The PC expansion coefficients can be calculated using the deterministic simulation results and least squares method.

We first express the spatial variation on material parameters and shape dimensions of several members of a railway track as Eqs. (7)-(11). The random numbers $\boldsymbol{\xi}^{(j)} = \{\boldsymbol{\xi}_E^{(j)}, \boldsymbol{\xi}_\rho^{(j)}, \boldsymbol{\xi}_A^{(j)}, \boldsymbol{\xi}_I^{(j)}, \boldsymbol{\xi}_X^{(j)}\}$ are introduced as

$$\begin{aligned}
&\boldsymbol{\xi}_E^{(j)} = \{\xi_{E,k}^{(i)} |\, k = 1, 2, \ldots, N_{KL}\}, \quad \boldsymbol{\xi}_\rho^{(j)} = \{\xi_{\rho,k}^{(i)} |\, k = 1, 2, \ldots, N_{KL}\},\\
&\boldsymbol{\xi}_A^{(j)} = \{\xi_{A,k}^{(i)} |\, k = 1, 2, \ldots, N_{KL}\}, \quad \boldsymbol{\xi}_I^{(j)} = \{\xi_{I,k}^{(i)} |\, k = 1, 2, \ldots, N_{KL}\},\\
&\boldsymbol{\xi}_X^{(j)} = \{\xi_{X,k}^{(i)} |\, k = 1, 2, \ldots, N_{KL}\},
\end{aligned} \tag{14}$$

where $j = 1, 2, \ldots N_{sim}$. The jth random numbers in Eq.(14) correspond to the jth rail material parameters $E_r^{(j)}(x)$, $\rho_r^{(j)}(x)$ and shape dimensions $A_r^{(j)}(x)$, $I_r^{(j)}(x)$ by Eqns.(7)-(11). Then all parameters and dimensions are deterministic. The jth wheel-rail contact force $P_i^{(j)}(t)$ $(i = 1, 2, \ldots, N_{wh})$, railpad force $F_{r,i}^{(j)}(t)$ $(i = 1, 2, \ldots, N_{slp})$ and sleeper-ballast force $F_{s,i}^{(j)}(t)$ $(i = 1, 2, \ldots, N_{slp})$ can be calculated using the FEM.

We next approximate the dynamic forces P_i, $F_{r,i}$ and $F_{s,i}$ with the Polynomial Chaos(PC) expansion as

$$\begin{aligned}
P_i(t, \boldsymbol{\xi}) &= \sum_{j=1}^{N_{PC}} P_{i,j}(t)\Phi_j(\boldsymbol{\xi}),\\
F_{r,i}(t, \boldsymbol{\xi}) &= \sum_{j=1}^{N_{PC}} F_{r,i,j}(t)\Phi_j(\boldsymbol{\xi}),\\
F_{s,i}(t, \boldsymbol{\xi}) &= \sum_{j=1}^{N_{PC}} F_{s,i,j}(t)\Phi_j(\boldsymbol{\xi}),
\end{aligned} \tag{15}$$

where $P_{i,j}$, $F_{r,i,j}$ and $F_{s,i,j}$ are the expansion coefficients on P_i, $F_{r,i}$ and $F_{s,i}$, respectively. Φ_j $(j = 1, 2, \ldots, N_{PC})$ is the polynomial chaos (PC), and is given by Hermite polynomials for normal random variables [15].

The PC expansion coefficients in Eq.(15) are defined as the solutions of the following linear algebraic equations by the least squares method:

$$\sum_{\beta=1}^{N_{PC}} \sum_{m=1}^{N_{sim}} \Phi_\alpha(\boldsymbol{\xi}^{(m)})\Phi_\beta(\boldsymbol{\xi}^{(m)})P_{i,\beta}(t) = \sum_{m=1}^{N_{sim}} P_i(t, \boldsymbol{\xi}^{(m)})\Phi_\alpha(\boldsymbol{\xi}^{(m)}) \tag{16}$$

$$\sum_{\beta=1}^{N_{PC}} \sum_{m=1}^{N_{sim}} \Phi_\alpha(\boldsymbol{\xi}^{(m)})\Phi_\beta(\boldsymbol{\xi}^{(m)})F_{r,i,\beta}(t) = \sum_{m=1}^{N_{sim}} F_{r,i}(t, \boldsymbol{\xi}^{(m)})\Phi_\alpha(\boldsymbol{\xi}^{(m)}) \tag{17}$$

$$\sum_{\beta=1}^{N_{PC}} \sum_{m=1}^{N_{sim}} \Phi_\alpha(\boldsymbol{\xi}^{(m)})\Phi_\beta(\boldsymbol{\xi}^{(m)})F_{s,i,\beta}(t) = \sum_{m=1}^{N_{sim}} F_{s,i}(t, \boldsymbol{\xi}^{(m)})\Phi_\alpha(\boldsymbol{\xi}^{(m)}) \tag{18}$$

where $\alpha = 1, 2, \ldots, N_{PC}$.

The expected values $\bar{P}_i$, $\bar{F}_{r,i}$ and $\bar{F}_{s,i}$ and the standard deviations σ_{P_i}, $\sigma_{F_{r,i}}$ and $\sigma_{F_{s,i}}$

Table 1: Expected value of the material parameters and shape dimensions of a rail.

$\bar{E}_{\mathrm{r}}$	210	(GPa)
$\bar{I}_{\mathrm{r}}$	3090×10^{-8}	(m^4)
$\bar{\rho}_{\mathrm{r}}$	7850	(kg/m^3)
$\bar{A}_{\mathrm{r}}$	77.50×10^{-4}	(m^2)
$\bar{X}$	0	(mm)

of the dynamic response $P_i(t)$, $F_{r,i}(t)$ and $F_{s,i}(t)$ are evaluated as follows:

$$\bar{P}_i(t) = P_{i,1}(t), \quad \sigma^2_{P_i}(t) = \sum_{m=2}^{N_{PC}} P^2_{i,m}(t), \tag{19}$$

$$\bar{F}_{r,i}(t) = F_{r,i,1}(t), \quad \sigma^2_{F_{r,i}}(t) = \sum_{m=2}^{N_{PC}} F^2_{r,i,m}(t), \tag{20}$$

$$\bar{F}_{s,i}(t) = F_{s,i,1}(t), \quad \sigma^2_{F_{s,i}}(t) = \sum_{m=2}^{N_{PC}} F^2_{s,i,m}(t), \tag{21}$$

In the present study, we apply Eqs.(15)-(21) to the simulation results at every time-marching step.

4 Influence of random variable selection on spatial variation of rail parameters to the dynamic response of railway track

In the present section, we investigate the influence of random variable selection on spatial variation of rail parameters to the dynamic response of a railway track, through numerical tests.

4.1 Problem description

We now simulate the vibration phenomena of the railway track with 11 sleepers and 0.56m sleeper spacing. The rail in the track is given by JIS 60kg rail. Table 1 shows the expected value of material parameters and shape dimensions of rail. The covariance kernel $C(x; y)$ on the spatial variation of rail parameters is defined as

$$C(x; y) = \sigma^2 \exp\left[-\frac{|x-y|}{b}\right] \tag{22}$$

where σ and b are standard deviations and correlation lengths on spatial variation. x and y are longitudinal coordinates of the rail. The eigenvalue λ and the eigenfunction

f are calculated by the following equation:

$$\int_\Omega C(x;\xi) f(x) d\Omega_x = \lambda f(\xi) \tag{23}$$

where Ω is a domain of a rail.

The spatial variation of Young's modulus E_r, the density ρ_r, the cross-sectional area A_r, the moment of inertia I_r and the surface profile X has 0.15mm correlation length. The standard deviations of E_r, ρ_r, A_r and I_r are prescribed to 10% of the expected value of these parameters, The standard deviation of the rail surface profile is 0.1mm. We now classify 5 material parameters and shape dimensions into 2 groups: (i) Young' modulus $E_r(x)$ and density $\rho_r(x)$ and (ii) cross-sectional area $A_r(x)$, moment of inertia $I_r(x)$ and rail surface profile $X(x)$. We assume that the two or three parameters in an every group are perfect correlation, and that the parameters in the different groups (e.g. the relation between $E_r(x)$ and $A_r(x)$) are mutually independent. The number of terms in the truncated KL expansion is prescribed into $N_{KL} = 5$. The 1st-order polynomial chaos is used for approximation of dynamic response in a probability space. The number of terms in the PC expansion is then $N_{PC} = 1 + 5 \times 2 = 11$. The sample number N_{sim} on the stochastic collocation method is set into 200.

In the present vibration analysis, the unsprung mass is $m_{wh} = 900$kg, and the dead load is $P_b = 45.57$kN. A wheel starts from the point of $x = 1.12$m, and runs at $c = 30$m/s (108km/h), 50m/s (180km/h), 70m/s (252km/h) or 90m/s (324km/h)on a rail. The rail pad in the present simulation has 50MN/m spring constant and 98kN sec/m damping coefficients. The sleeper mass is 130kg. In voigt units on the sleeper-ballast force, a spring constant is 84MN/m and a damping coefficients is 98kN sec/m.

4.2 Wheel-rail contact force

Figure 2 illustrates the expected value and the standard deviation of the wheel-rail contact force at each wheel position x. The wheel-rail contact force follows the normal- or the log-normal distribution because the 1st-order polynomial chaos is used for approximation in a probability space. The amplitude of the expected value of the wheel-rail contact force increases with speed-up of wheel running. The amplitude for 30m/sec is about 4kN, while the one for 90m/sec is more than 10kN. The standard deviation shows about 5% value of the expected value in initial stage of the wheel running due to transient response, and subsequentially decreases to about 1% of the expected value. A higher speed on wheel running leads to a larger standard deviation: the one for $c = 90$m/sec shows 20% value of the expected value. The dynamic behavior on the expected value and the standard deviation tends to be independent of the choice of the standard normal- or the standard log-normal random variables in KL expansion.

4.3 Railpad force

Figure 3 illustrates the expected value and the standard deviation of No.6 railpad force $F_{rp,6}$ at each wheel position x. The railpad force is defined as the rail-sleeper force.

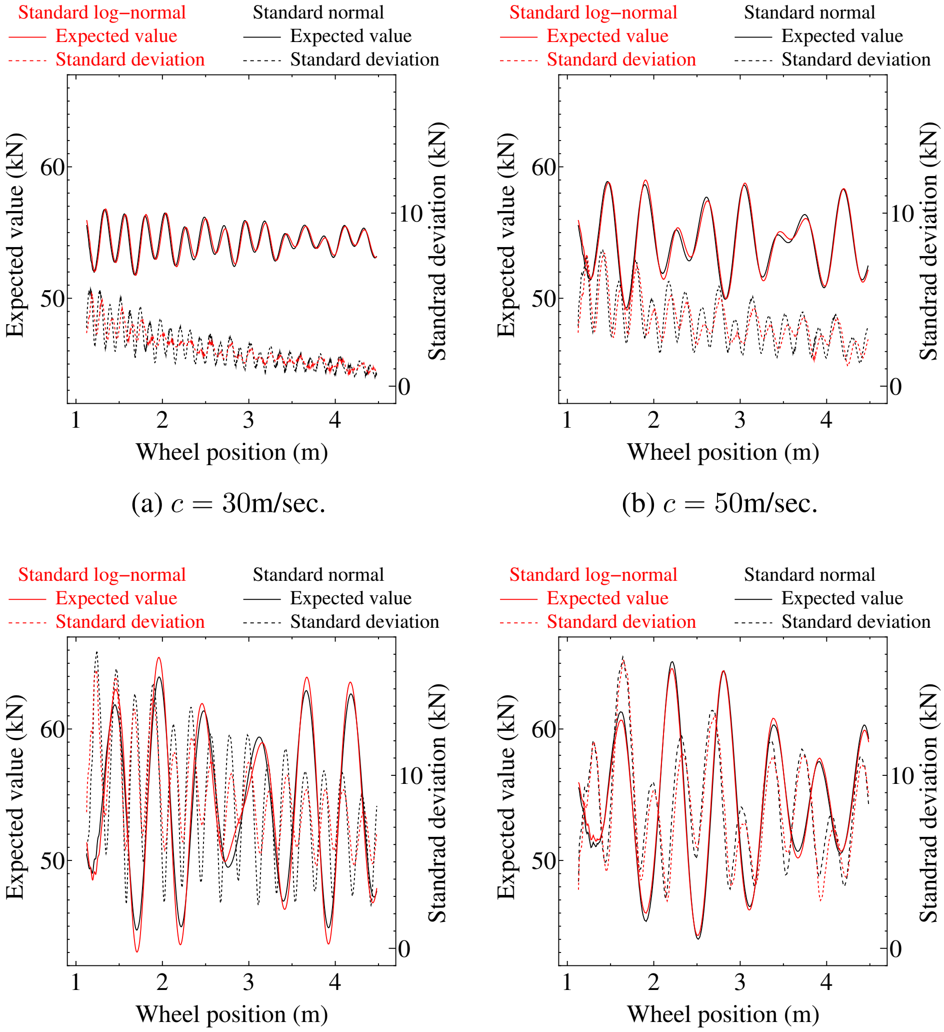

(a) $c = 30$m/sec.

(b) $c = 50$m/sec.

(c) $c = 70$m/sec.

(d) $c = 90$m/sec.

Figure 2: Expected value and the standard deviation of the wheel-rail contact force P_1 at each wheel position x.

The No.6 sleeper locates the center of the model track with 11 sleepers. The railpad force follows the normal- or the log-normal distribution because the 1st-order polynomial chaos is used for approximation in a probability space. The maximum of the expected value of the railpad force tends to increase with rise of the wheel running speed c. The maximum force for $c = 90$m/sec shows the 110% of the maximum for the lowest speed $c = 30$m/sec in the present simulation. The standard deviation of the railpad force also rises with wheel speed increase. While the standard deviation for $c = 30$m/sec is about 5% of the expected value of $F_{rp,6}$, the one for 90m/s amplifies to 25% of the expected value. The choice of the random variables in KL expansion have no effect on this tendency.

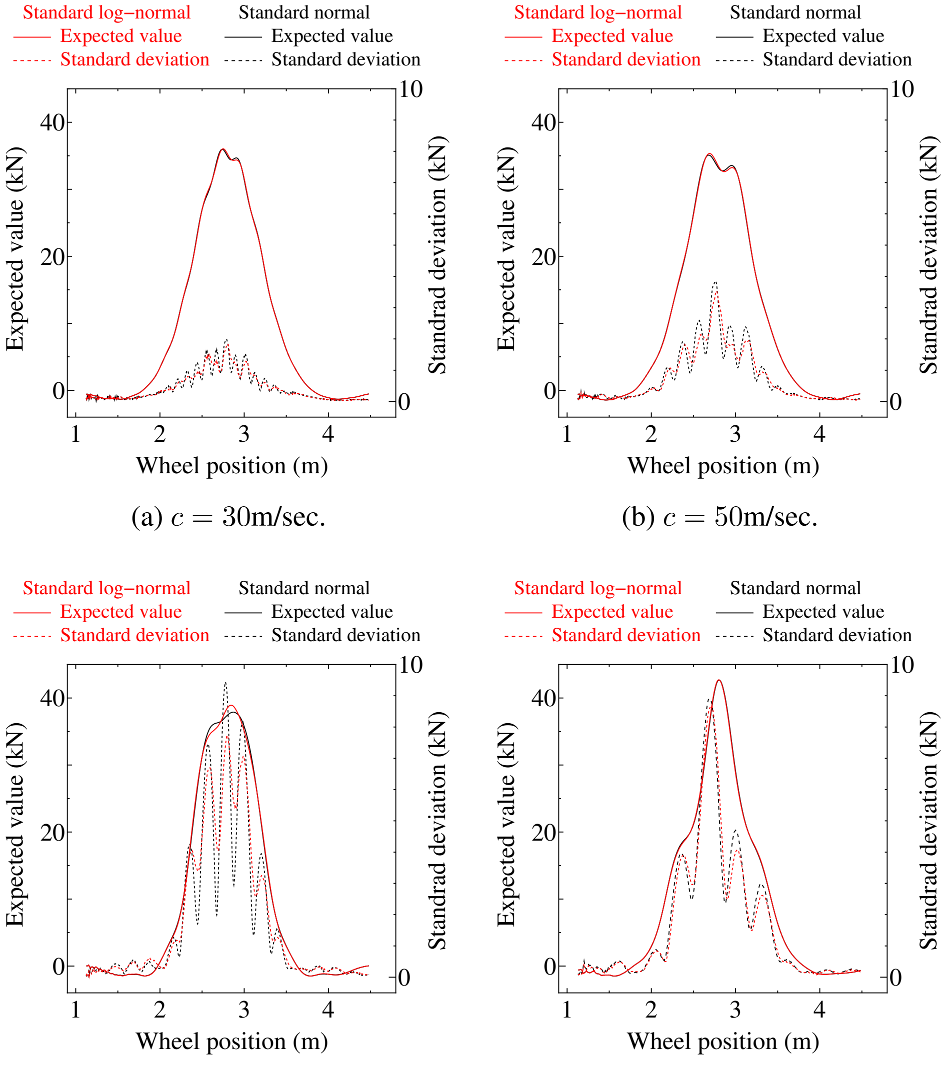

(a) $c = 30$m/sec. (b) $c = 50$m/sec. (c) $c = 70$m/sec. (d) $c = 90$m/sec.

Figure 3: Expected value and the standard deviation of the No.6 railpad force $F_{rp,6}$ at each wheel position x.

4.4 Sleeper-ballast force

Figure 4 illustrates the expected value and the standard deviation of the wheel-rail contact force on the No.6 sleeper at each wheel position x. The sleeper-ballast force follows the normal- or the log-normal distribution because the 1st-order polynomial chaos is used for approximation in a probability space. The dynamic behavior of the expected value and the standard deviation of the sleeper-ballast force shows shimilar tendency of the railpad force. The simulation results for the standard log-normal random variables in KL expansion is similar to those for the standard normal random variables.

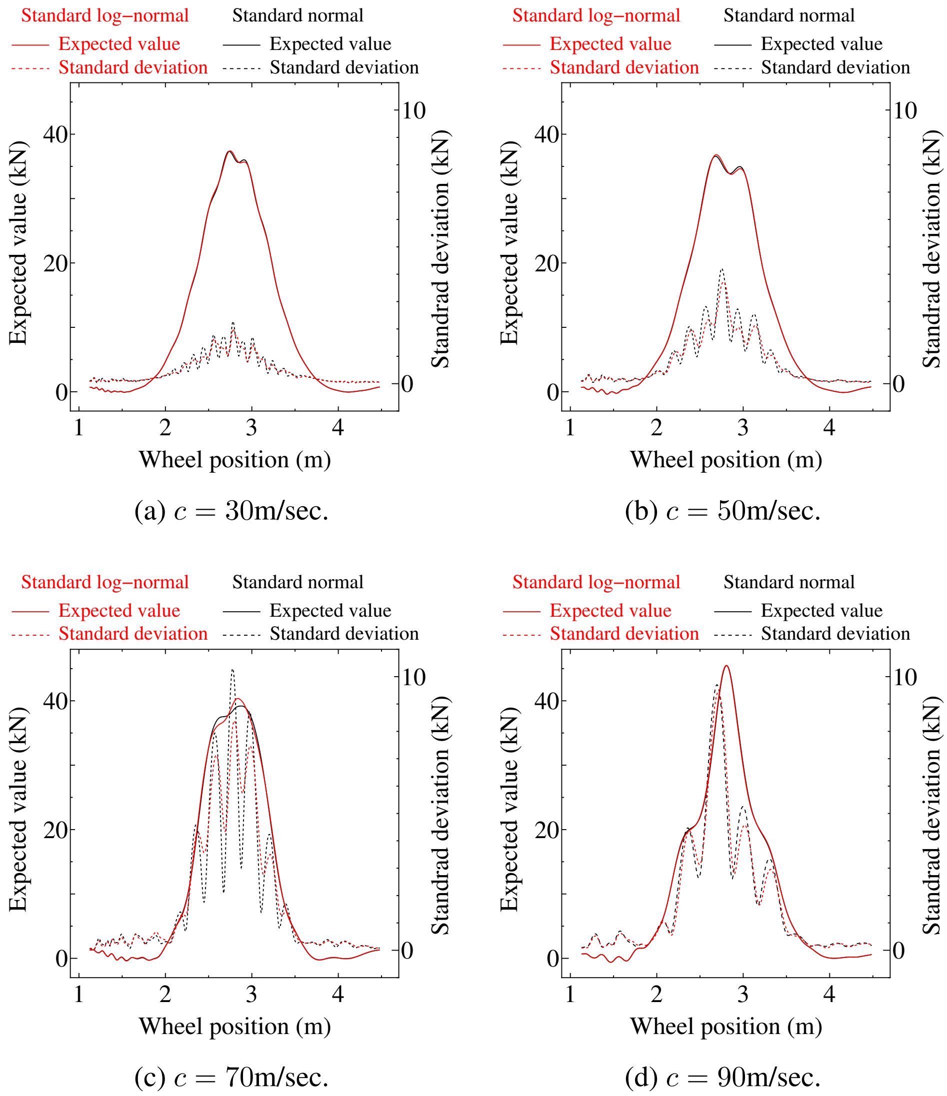

(a) $c = 30$m/sec.

(b) $c = 50$m/sec.

(c) $c = 70$m/sec.

(d) $c = 90$m/sec.

Figure 4: Expected value and the standard deviation of the No.6 sleeper-ballast force $F_{s,6}$ at each wheel position x.

5 Concluding remarks

In the present paper, we have investigated the influence of random variables selection on spatial variation of rail material parameters and shape dimensions to the expected value and the standard deviation of the simulated track dynamic response. The well known beam-mass-spring system [2] was used as the wheel-track vibration model. The spatial variation was considered about Young's modulus, density, cross-sectional area, moment of inertia and surface profile on a rail. The Karhunen-Loève (KL) expansion was used for modeling the spatial variation of these rail parameters. We have considered a choice of the random variables in the KL expansion, the standard normal- and the standard log-normal random variables. The dynamic response in probability space is evaluated using the polynomial chaos (PC) and the stochastic collocation method.

In our simulation, we investigate the expected value and the standard deviation of the three kinds of dynamic forces, the wheel-rail contact force, the railpad force and the sleeper-ballast force for several running speed (30, 50, 70 and 90 m/sec) of a wheel. The expected value and the standard deviation of the wheel-rail contact force increase with rise of the wheel running speed c, due to existance of rail surface profile. The standard deviation for $c = 90$ m/sec shows 20% of the expected value. The standard deviations of the railpad force and the sleeper-ballast force clearly rise from 5% of the expected values of them for $c = 30$ m/sec to about 25% for $c = 90$ m/sec.

The dynamic behavior on the expected value and the standard deviation tends to be independent of the choice of the standard normal- or the standard log-normal random variables in KL expansion.

Acknowledgements

This work was supported by JSPS KAKENHI Grant Number JP22K04282.

References

[1] Knothe, K.L. & Grassie, S.L.: Modelling of railway track and vehicle/track interaction at high frequencies. *Vehicle Sys. Dyn.*, Vol.22, pp.209-262, 1993.

[2] Koro, K., Abe, K., Ishida, M. & Suzuki, T.: Finite element simulation of the field test on the railway track with rail joints. *J. Appl. Mech. JSCE*, Vol.8, pp.1037-1047, 2005 (in Japanese).

[3] Perrin, G., Soize, C., Duhamel. D. & Funfschilling, C.: Track irregularities stochastic modeling. *Prob. Eng. Mech.*, Vol.34, pp.123-130, 2013.

[4] Hofer, V. & Bach, H.: Statistical monitoring for continual quality control of railway ballast. *Expert Sys. with Appl.*, Vol.42, pp.8557-8572, 2015.

[5] Navikas, D., Sivilevicius, H. & Bulevicius, M.: Investigation and evaluation of railway ballast properties variation during technological processes. *Const. Build. Mat.*, Vol.185, pp.325-337, 2018.

[6] Germonpre, M., Nielsen, J.C.O., Degrande, G. & Lombaert, G.: Contributions of longitudinal track unevenness and track stiffness variation to railway induced vibration. *J. Sound & Vib.*, Vol.417, pp.292-307, 2018.

[7] Xu, L., Zhai, W., Gao, J., Meacci, M. & Chen, X.: On effects of track random irregularities on random vibrations of vehicle-track interaction. *Prob. Eng. Mech.*, Vol.50, pp.25-35, 2017.

[8] Andersen, L. & Nielsen, S.R.K.: Vibration of a track caused by variation of the foundation stiffness. *Prob. Engrg. Mech.*, Vol.18, pp.171-184, 2003.

[9] Bressolette, Ph., Fogli, M. & Chauviere, C.: A stochastic collocation method for large classes of mechanical problems with uncertain parameters. *Prob. Eng. Mech.*, Vol.25, pp.255-270, 2010.

[10] Rhayma, N., Bressolette, Ph., Breul, P., Fogli, M. & Saussine, G.: A probabilistic approach for estimating the behavior od railway tracks. *Eng. Struct.*, Vol.33, pp.2120-2133, 2011.

[11] Sadri, M., Lu, T. & Steenbergen, M.: Railway track degradation: The contribution of a spatially variant support stiffness - Global variation. *J. Sound & Vib.*, Vol.464, Art.114992, 2020.

[12] Watanabe, A. & Koro, K.: Influence of spatial variation of elastic modulus of ballast material on vibration response of a ballasted railway track. *J. Appl. Mech., JSCE*, Vol.72(2), pp.I_265 - I_276, 2017 (in Japanese).

[13] Koro, K. & Abe, K.: Wheel-track vibration analysis of ballasted track with spatial variation of ballast material parameters. *J. Railway Eng. JSCE*, Vol.25, pp.225-232, 2021 (in Japanese).

[14] Koro, K. & Abe, K.: Influence of spatial variation of several parameters of rail on simulated wheel-track dynamic response. *J. JSCE*, Vol.79, No.15, 22-15027, 2023 (in Japanese).

[15] Ghanem, R.G. & Spanos, P.G.: Stochastic finite elements. Dover, 1991.

[16] Achharjee, S. & Zabaras, N.: A non-intrusive stochastic Galerkin approach for modeling uncertainty propagation in deformation process. *Comp. & Struct.*, Vol.85, pp.244-254, 2007.

[17] Honda, R. & Ghanem, R.: Spectral stochastic finite element method for lognormal uncertainty. *J. Appl. Mech., JSCE*, Vol.7, pp.391-398, 2004.